Proceedings of the 1st International

Conference on Ageing of Materials & Structures

Delft University of Technology

www.ams.tudelft.nl

ams-citg@tudelft.nl

Editors:

K. van Breugel, E.A.B. Koenders

Cover:

I.B. Design

Probabilistic corrosion forecasting of steel in concrete with potential-dependent chloride threshold

Andrea N. Sánchez[1*], Alberto A. Sagüés[1]
(1) University of South Florida, Tampa, Florida, USA

Abstract: The concrete chloride corrosion threshold depends on the passive steel. Inclusion of potential dependence of threshold (PDT) requires adaptive modelling, where effects of prior activation events on corrosion and potential throughout the structure are modelled at each time step. Previous work showed that PDT leads to slower long term predicted damage development than with traditional potential-independent threshold (PIT) models. The paper expands the modelling approach to probabilistically distributed surface chloride content and concrete cover. Instances are revealed where PDT can also result in earlier onset of damage compared with PIT predictions, reverting to the previously established long term behaviour later on as the system ages. The results underscore the importance of considering PDT in modelling forecasts for ageing structures.

Keywords: Corrosion, concrete, forecasting, chloride threshold, modelling

1 Introduction

The corrosion-related service life of a reinforced concrete structural element exposed to a chloride rich environment is obtained as the sum of the durations of the initiation and propagation stages. The initiation stage starts when the structure is put in service and ends when the critical chloride corrosion threshold C_T on the steel bar surface is exceeded. At this point, the propagation stage begins where expansive corrosion products accumulate on the steel surface. The propagation stage ends when surface cracking or other given limit state is reached. Often, the time-length of the initiation stage is longer than that of the propagation stage; hence the former receives more attention in the literature.

Many of the durability models available assume a system with time-invariant C_T typically within the range of 0.2 and 0.5% by weight of cement. Investigations to determine the value of C_T have reported values that depend on type of cement, the area of steel, the concrete-steel interface, the pore network pH, and the steel potential while in the passive condition. [1-3] Despite the limited amount of work reported on the latter, findings suggest that for $E < \sim -0.2$ V (SCE)[1] the C_T value increases significantly. [3-7]. In that domain the relationship between C_T and E value is reported to approximately follow:

$$C_T = C_{T0}10^{\left(\frac{E_{T0}-E}{\beta_{CT}}\right)} \quad \text{for E<-0.250 V (SCE)} \qquad (1)$$

Where C_{T0} is the C_T value at a reference potential E_{T0}, and β_{CT}, named the cathodic prevention slope, is indicative of the extent to which E needs to be decreased to achieve a given relative increase in C_T. Recent work suggests that the upper bound of β_{CT} is in the order of -0.55 V per decade of chloride concentration. [3,7].

A recent deterministic computational model incorporated a potential-dependent-threshold (PDT) per Eq. (1) in an innovative damage estimation approach that integrates the initiation and propagation stage in a single model [5,8]. The model updates the macrocell current and potential distribution of the system as new regions of the reinforcing steel assembly become active, and

* Corresponding author affiliation and e-mail address
[1] Steel potential with respect to a Saturated Calomel Electrode (SCE)

determines how C_T evolves in the still passive regions, adjusting the timing of subsequent corrosion initiation events accordingly. In that previous work the model was implemented for a marine reinforced concrete column partially submerged in seawater with an invariant chloride diffusivity D and concrete cover X_C. The surface chloride concentration C_S, concrete resistivity ρ and oxygen diffusivity D_{O2} profiles varied systematically and uniformly with elevation following typical marine service trends. Cases where C_T was independent of E were also modelled for comparative purposes. The concrete deterioration was quantified as a damage function of time. The cases with PDT resulted in a dramatically reduced damage projection at long service times compared to the time-invariant C_T cases, highlighting the importance of considering PDT in a damage-prediction model. However, those introductory calculations were deterministic, with systematic but not random variation of key parameters. The random variation is more likely to be representative of actual systems. The objective of this paper is to expand the previous modelling approach to explore the effect of incorporating PDT on damage projections for a system with randomly distributed profiles of selected corrosion determining parameters.

2 System Details

2.1 Modelled system and investigated cases

The system modelled is comparable to that simulating a partially submerged marine column described in Refs [5,8]. However, in this paper only the atmospheric portion of the column was considered as illustrated in Figure 1. Using a simplified one-dimensional approach, the column is divided into 101 elements along the length L of the column with diameter ϕ. The model parameters and input values are indicated in Table 1.

Previous versions of this modelling approach were deterministic with smoothly elevation-variant concrete resistivity, surface concentration, oxygen diffusivity and chloride diffusivity. In this investigation, random pattern profiles (Figure 1) without systematic overall trends were implemented for the chloride surface concentration and the concrete cover. The profiles were created using a random number generator and modified to minimize short wavelengths variations. Typical average and standard deviation values found in Florida marine structures [9] were assigned to each profile (Table 1).

At first, the entire system is passive and the chloride ions ingress through the concrete pore network. Later on, active corrosion starts, first at regions with the most adverse combinations of chloride surface concentration and low cover. The corrosion evolution of the system is calculated at every time step by three modules. The Chloride Transport Module is based on calculating the amount of chloride ion ingress through the concrete and accumulating at the steel bar surface, assuming simple Fickian diffusion. When the chloride ion concentration at the steel bar exceeds the C_T value at that location the steel changes from passive to active state. Corrosion macrocells are then generated between the active and the passive regions, causing a change from the initial potential distribution. The Corrosion Distribution Module computes at each time step the distribution of potentials and macrocell currents through the concrete domain, linking those with the boundary conditions at the steel surface according to the assumed polarisation parameters for the corrosion reactions. The C_T elevation profile is likewise updated accordingly per Eq. (1), so initiation events at subsequent time steps are ruled by the continually updated threshold profiles. Lastly, the Surface Damage Evaluation Module tracks and integrates the local corrosion rate at the active steel elements, yielding a local corrosion penetration that accumulates until it reaches a critical limit P_{CRIT}[10] (Table 1) at which point local damage is declared. The number of damaged elements is tallied as a percentage of the total number of elements as function of time, and reported as the damage function of the system.

For this exploratory study random variability was limited to the values of Cs and Xc, in two case classes in which only one of each respectively was varied, and another case class where

both varied simultaneously. All other system parameters were kept constant. Each of those scenarios was implemented to obtain damage functions for low and high uniform concrete resistivity ρ situations (with consequently strong and weak macrocell coupling situations), for a total of six case classes each incorporating PDT, as well as similar set of control calculations with potential-independent threshold (PIT). Each class calculation was replicated with multiple randomizations.

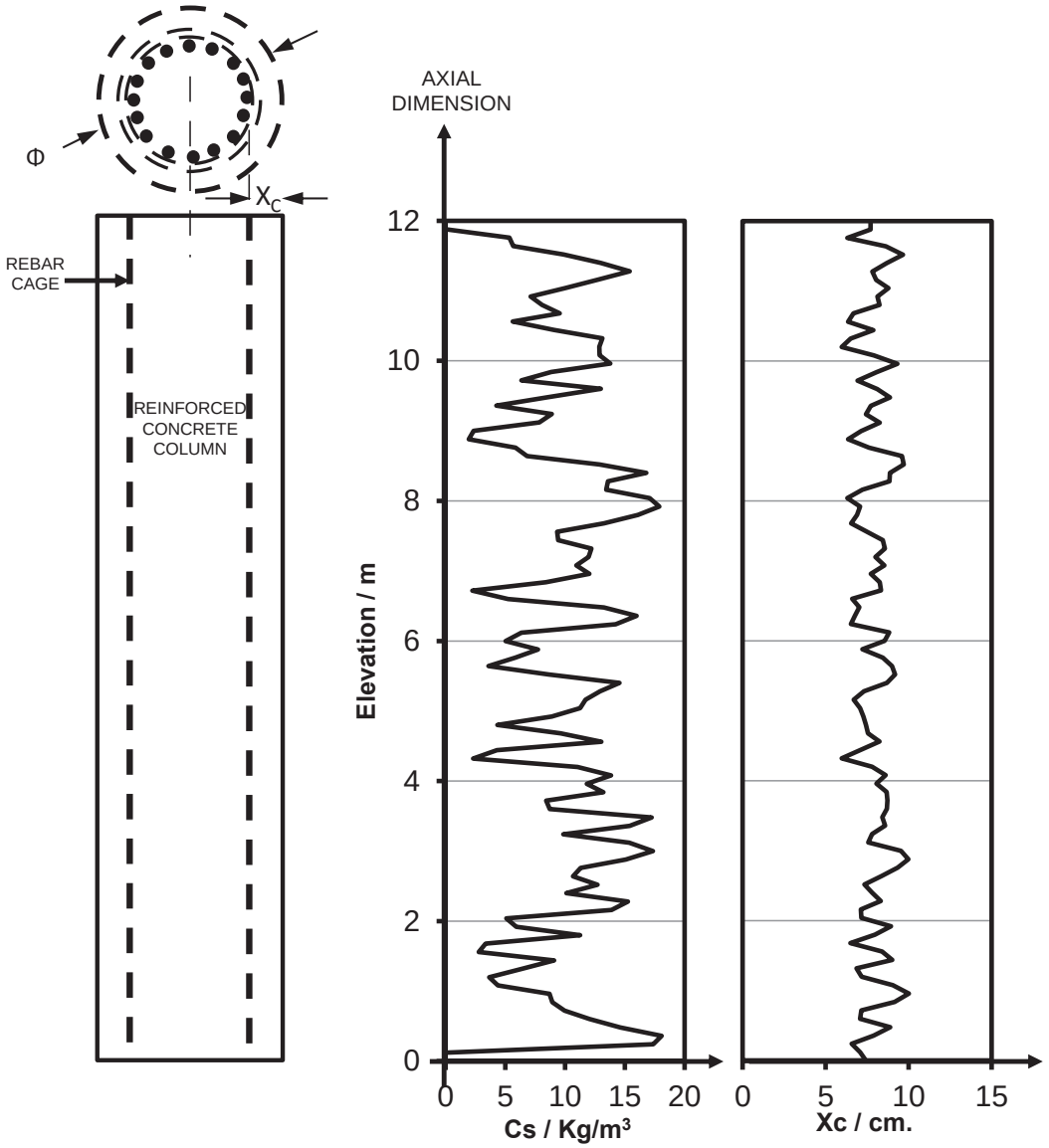

Figure 1 Left: System modeled. Right : Representative randomly distributed profiles for the surface concentration and concrete cover.

Table 1 Model Parameters

Column diameter	Φ=	105 cm	
Column Length	L=	1200 cm	
Steel Cover (average)	Xc_{avg} =	8 cm	
Steel Cover (standard deviation)	Xc_{std} =	2 cm	
Cl- Surface Conc. (average)	Cs_{avg}=	10,4 Kg/m3	
Cl- Surface Conc.(standard deviation)	Cs_{std}=	4,5 Kg/m3	
Concrete Resistivity	ρHigh=	7,5 104 ohm-cm	
	ρLow=	1,5 104 ohm-cm	
Oxygen Diffusivity	DO_2=	2,510-5 cm2/sec	
Chloride Diffusivity	D_{Cl-}=	2,5 10-8 cm2/sec	
O2 Surface Concentration	Cs_O=	2,5 10-7 mol/cm3 (in pore water)	
Chloride Threshold Parameters			
	C_{To}=	1,78 Kg/m3	
	E_p=	-0,100 mV	
	β_{CT} =	0,550 V/decade	
Polarisation Parameters	E_0 (-V CSE)	i_0 (A/cm2)	Tafel Slope (V)
Iron Dissolution	-0,780	1,875 10-8	0,06
Oxygen Reduction	0,16	6,25 10-10	0,16
Steel Current Density (passive condition)	i_p=	0,058 10-6 A/cm^2	
Critical Corrosion Penetration	P_{CRIT}=	0,01 cm	

3 Results and Discussion

Results presented are from one realization each, but representative of the trends obtained with multiple realizations of the random variable distributions. Figure 2 illustrates a typical output, showing potential and corrosion current elevation profiles for the PDT and PIT cases with randomly distributed Xc and low r. The first two activation events occurred at 12.5 years, manifested by local negative potential shifts and the transition from passive current density ip to a higher active iron dissolution value at each active spot. By year 13.5 the system with PIT had two more active spots, but no new activation was observed in the PDT case. By year 15 twelve activation events already took place for PIT compared to five activations for PDT. As expected, less activation events were present in the PDT case as a result of the increase of the C_T by the negative drop of E in the passive areas adjacent to the active spots.

For the same case described above, the corrosion charge per area of each active element in a 75 year period is shown in Figure 3. The top and the bottom figures correspond to the PIT and PDT scenarios, respectively. The horizontal dashed line indicates the faradaic conversion equivalent to P_{CRIT}, which corresponds to 270 C/cm2. Concrete damage is declared when the solid lines cross the dashed line.

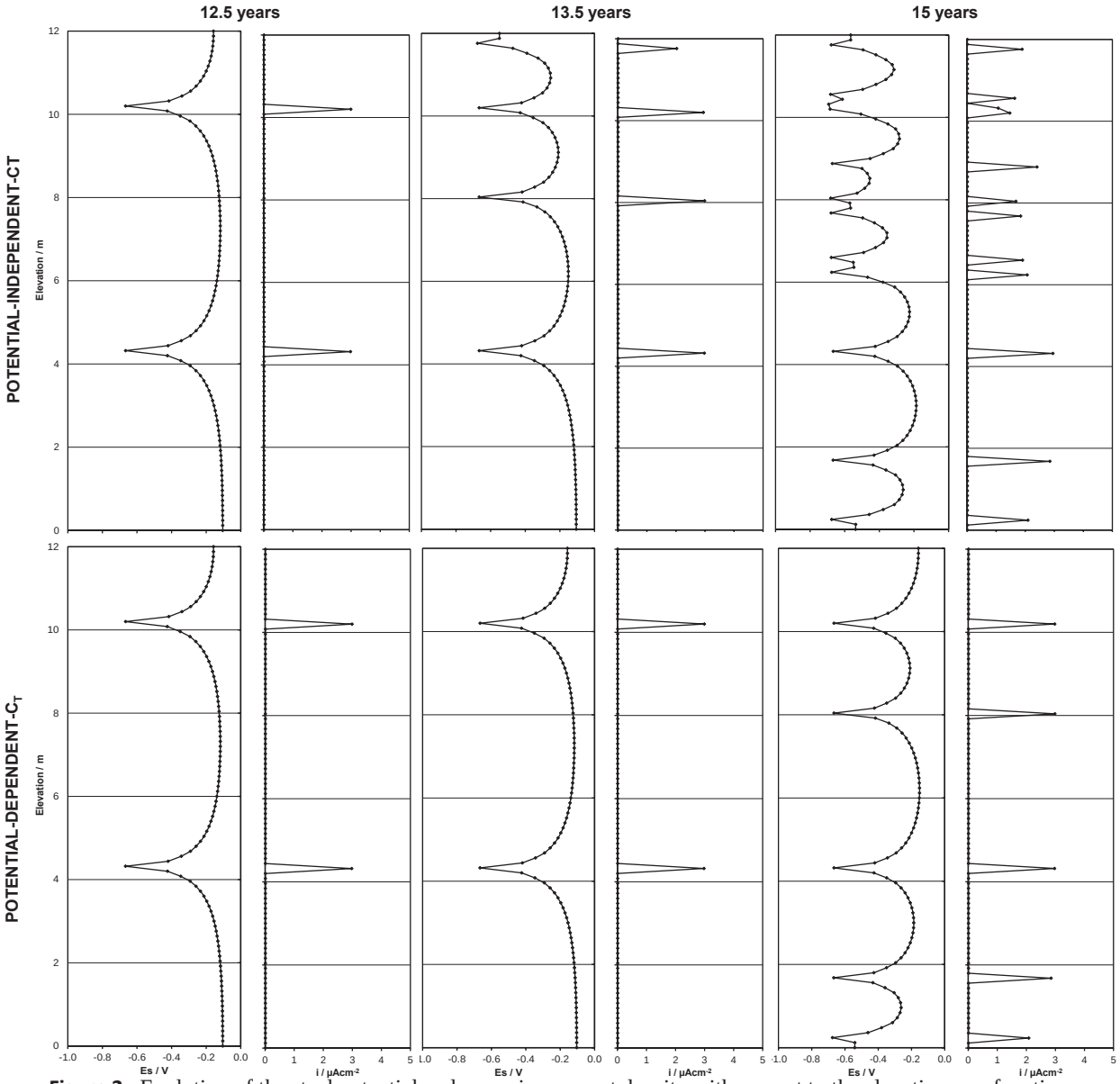

Figure 2: Evolution of the steel potential and corrosion current density with respect to the elevation as a function of time for the random distributed concrete cover with low resistivity

The damage function for the system, expressed as the total count of damaged elements (each corresponding to about 0.39 m^2 of external column surface) as function of time is exemplified for all case classes examined in Figure 4. Multiple realizations with the same averages and variances of the distributed parameters, but with different random assignments, yielded damage functions not deviating much from those exemplified in the figure.

The results share features seen in the earlier work [5, 8] with systematic instead of random parameter variability. Most noteworthy is the much reduced (by factors ranging from ~2 to ~5) damage projection for the PDT compared to the PIT cases at greater structure ages. That behaviour is the direct result of the delay, and sometimes suppression, of new activation events as the potential of the remaining passive part of the steel becomes increasingly more negative with time with consequent elevation of C_T there. That delay/suppression is easily observed in Figure 2, where the initial activation sequence does not vary much between the PDT and PIT scenarios but strong differentiation emerges later with much fewer activation events in the PDT case. Figure 3 conveys the same message over a longer time frame. The results further confirm

earlier conclusions indicating that this differentiation, presently ignored in most analyses, should be incorporated in advanced models of damage forecasts for aged structures. Not surprisingly, within a given assumed condition (PIT or PDT) the cases with the lower concrete resistivity projected earlier damage than in those for the higher resistivity, since the latter results in lowered macrocell action and hence slower corrosion at the active spots..

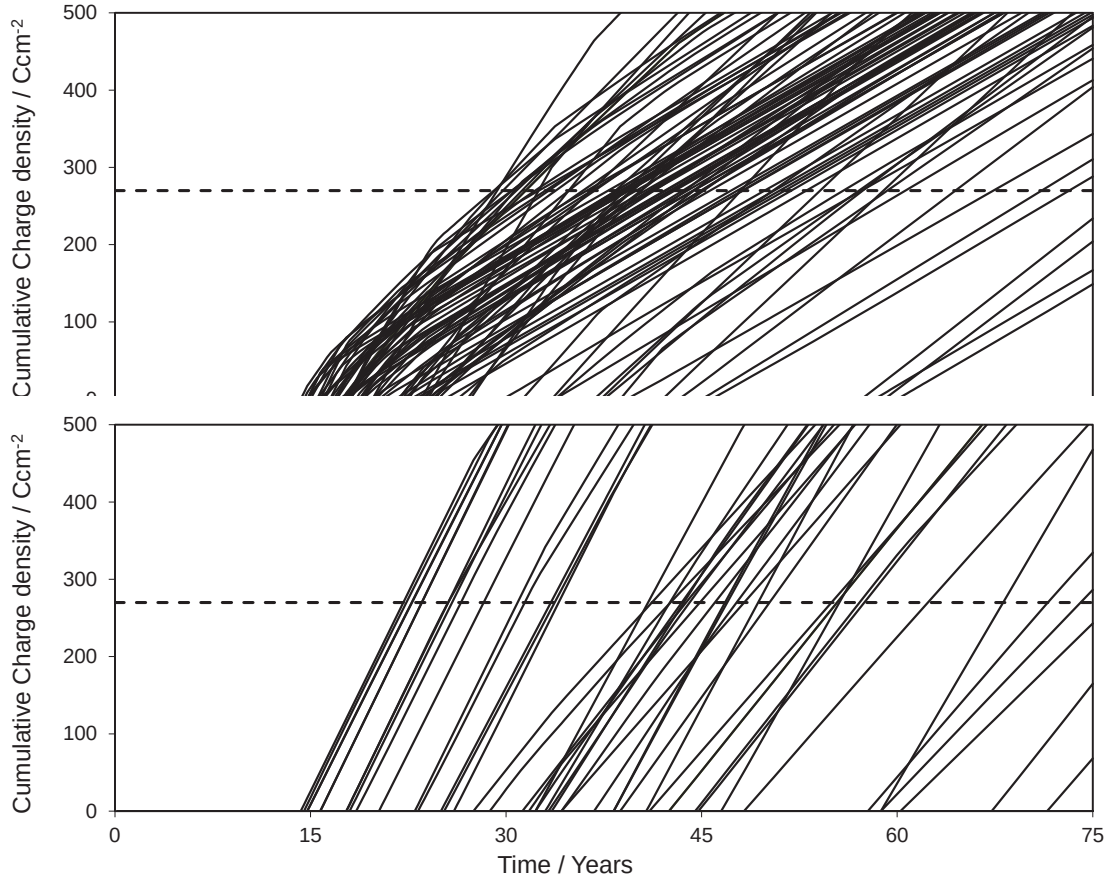

Figure 3: Cumulative corrosion charge density as a function of time for the randomly distributed Cs with high resistivity. Top: Potential-independent-threshold case. Bottom: Potential-dependent-threshold case. Dashed line corresponds to the critical penetration condition.

A notable feature in the present work is that introduction of random parameter fluctuations revealed some instances of significantly greater *early* damage projections in the PDT than in the corresponding PIT cases of the same resistivity. This feature was not readily apparent in the previous analyses with systematic and uniform variation of parameters with elevation.[5, 8] As shown in Figure 4, the earlier damage development in PDT sometimes started as much as ~7 years earlier than for PIT. These instances are a propagation stage phenomenon and, paradoxically, a result of the delay in other activation events following the first ones. That delay enables sustained macrocell enhancement of the early active regions with consequent faster local corrosion rates for those few regions, and their early declarations of damage. In contrast, for PIT the rate of appearance of new active regions is not decreased and thus the remaining cathodic portion of the steel assembly has to support an increasing number of anodes, with consequent less enhancement of their corrosion rate and slower arrival of the damage declarations. The corrosion charge curves in Figure 3 are consistent with this interpretation, showing that the fewer PDT propagation events have a greater slope than the more numerous cases for PIT. As time progresses, the extent of macrocell action per active region decreases and the system tends toward smaller, and increasingly diffusion-limited, cathodically controlled

regimes in both cases. At longer service times, the damage accumulation for PIT eventually overcomes that of PDT with the long-term trend differences noted earlier.

The increased early damage progression for PDT relative to PIT was not observed in all instances, and it is likely to depend on the variability of the parameters chosen to capture the nonuniformity of external aggressive agents and concrete cover and properties. The more uniform, systematic parameter profiles used in the earlier simulations [5, 8] tended to mask this outcome through the timing of new activation events. Continuation research is in progress to determine the sensitivity of that behaviour to assumed parameter distributions.

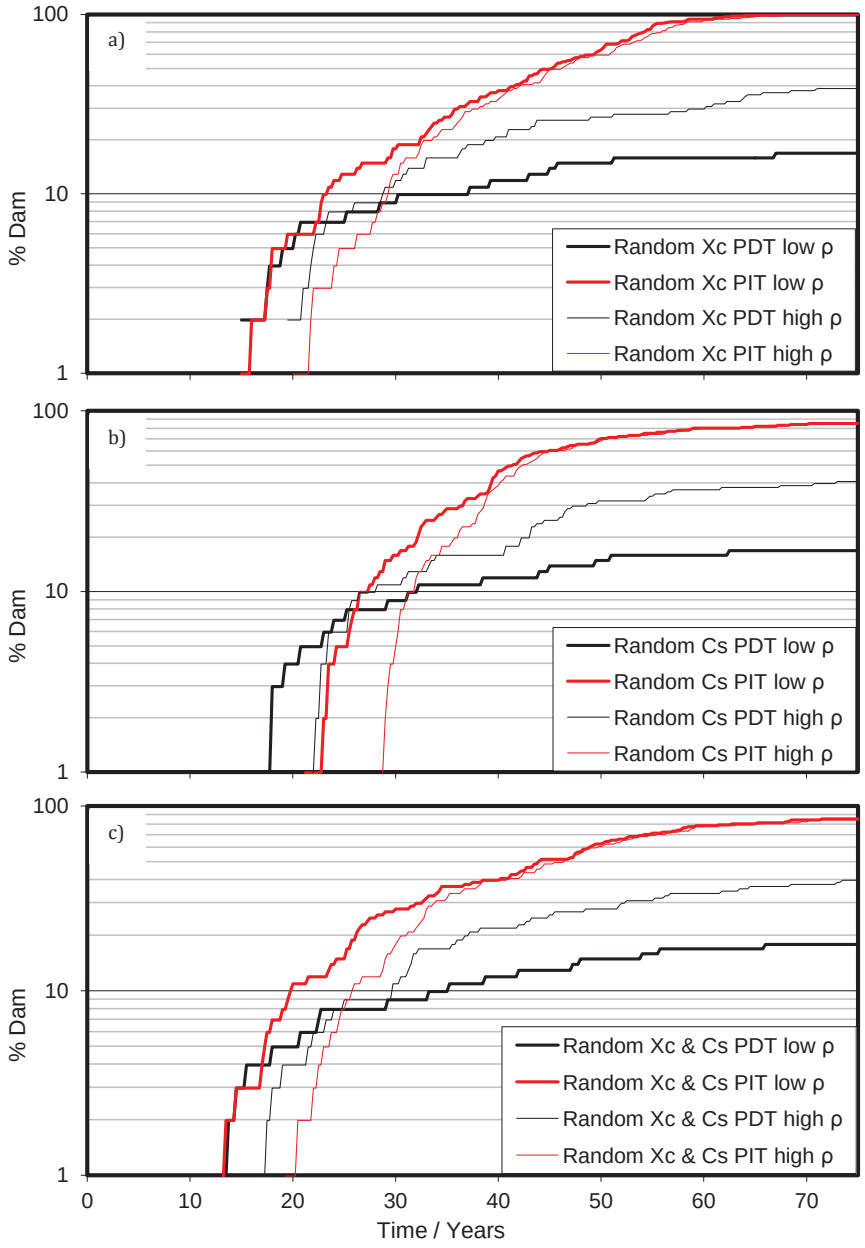

Figure 4 Damage progressions for all cases. a) Randomly distrbuted Xc. b) Randomly distrbuted Cs. c) Combined case

4 Conclusions

An innovative corrosion damage forecasting approach for corrosion of steel in concrete was implemented, where the initiation and propagation stages were effectively merged in a single

damage forecast model, including potential-dependent-chloride threshold (PDT), and extending previous work to include probabilistically distributed chloride surface concentration and the concrete cover. Traditional potential-independent threshold (PIT) cases were calculated for comparison.

The results were consistent with previous work in systems with systematic parameter variations, showing that long-term damage was strongly reduced or delayed for PDT cases compared to the PIT controls. The reduction is due to the suppression or delay of corrosion initiation events due to the polarisation of the remaining steel assembly toward more negative potentials as more active regions develop, thus increasing the value of the corrosion threshold.

The probabilistic calculations revealed however situations, not evident in previous work, where accounting for PDT actually resulted in more early damage events than with PIT, with the opposite long term trend noted above developing later on. The finding was ascribed to a propagation stage phenomenon, where the fewer active regions present under PDT experience greater localised macrocell-induced corrosion than the more numerous regions under PIT.

The results underscore the importance of considering PDT in the forecast of corrosion in ageing reinforced concrete structures.

5 Acknowledgements

This work was supported by the State of Florida Department of Transportation and the U.S. Department of Transportation. The findings and opinions presented here are those of the authors and not necessarily those of the supporting organizations.

6 References

[1] Pedeferri, P. (1996). Cathodic protection and cathodic prevention. Construction and Building Materials, 10(5), 391-402.

[2] Angst, U., Elsener, B., Larsen, C. K., & Vennesland, Ø. (2009). Critical chloride content in reinforced concrete—a review. Cement and Concrete Research,39(12), 1122-1138.

[3] Alonso, C., Castellote, M., & Andrade, C. (2002). Chloride threshold dependence of pitting potential of reinforcements. Electrochimica Acta, 47(21), 3469-3481.

[4] Presuel-Moreno, F. J., Sagüés, A. A., & Kranc, S. C. (2005). Steel activation in concrete following interruption of long-term cathodic polarization. Corrosion,61(5), 428-436.

[5] Sagüés, A.A., Kranc, S.C. & Lau, K.(2009) Service Life Forecasting for Reinforced Concrete Incorporating Potential-Dependent Chloride Threshold, in NACE Corrosion 2009, Atlanta, GA. NACE International, p. 22.

[6] Sánchez, A.N. & Sagüés, A.A. (2012) Chloride Threshold Dependence on Potential in Reinforced Mortar. Paper No. 1728 in NACE Corrosion 2012. Salt Lake City, UT. NACE International, pp. 11.

[7] Sánchez, A.N. & Sagüés, A.A. (2014) Chloride Corrosion Threshold Dependence on Steel Potential in Reinforced Concrete. Paper No. 4118 in NACE Corrosion 2014. San Antonio, TX. NACE International, pp. 10.

[8] Sánchez, A.N., & Sagüés, A.A. (2013) Potential-Dependent Chloride Threshold in Reinforced Concrete Damage Prediction – Effect of Activation Zone Size. Paper No. 2704 in NACE Corrosion 2013. Orlando, FL. NACE International, pp.14

[9] Sagüés, A. A. (2003). Modeling the effects of corrosion on the lifetime of extended reinforced concrete structures. Corrosion, 59(10), 854-866.

[10] Torres-Acosta, A. A., & Sagüés, A. A. (2004). Concrete Cracking by Localized Steel Corrosion--Geometric Effects. ACI Materials Journal, 101(6).